

Synchronization Patterns Generated in Globally Cross-Coupled Chaotic Circuits

Yumiko Uchitani[†] and Yoshifumi Nishio[‡]

Department of Electrical and Electronic Engineering, Tokushima University
 2-1 Minami-Josanjima, Tokushima, 770-8506 JAPAN
 Email: {uchitani, nishio}@ee.tokushima-u.ac.jp

Abstract—In this study, synchronization patterns generated in globally cross-coupled chaotic circuits are investigated. Computer simulations and circuit experiments show that this coupled system produces several phase patterns.

1. Introduction

Many people have been trying to develop some applications to information processing by exploiting oscillatory phenomena in neural networks. Such neural networks can produce some kinds of phase patterns, and they may be utilized for associative memory or image processing [1][2].

On the other hand, since synchronization phenomena in coupled chaotic systems are good models to describe various higher-dimensional nonlinear phenomena in the field of natural science, studies on synchronization phenomena in such systems are extensively carried out in various fields [3][4].

In our past studies [5]-[7], we investigated the state transition phenomenon in two cross-coupled chaotic circuits and the phase patterns characterized by synchronization in a ring of cross-coupled chaotic circuits. The interesting state transition phenomenon and various synchronization phenomena including quadrature-phase synchronization are inherent in our coupled model.

In this study, we consider a globally coupled model based on the cross-coupled chaotic circuits and investigate the synchronization patterns characterized by various synchronization modes in the coupled system. Computer simulations and circuit experiments for the case of three and four subcircuits cases show that the proposed coupled system produces several synchronization patterns.

2. Basic Circuit [5][6]

In this section, we review the phenomena observed from simple two cross-coupled chaotic circuits. Figure 1 shows the basic circuit model. In this model, two simple autonomous chaotic circuits [8][9] are cross-coupled via inductors L_2 .

The circuit equations are given as follows.

$$\begin{cases} \dot{x}_k = z_k \\ \dot{y}_k = \alpha\{\gamma y_k - w_k - \beta f(y_k - z_k)\} \\ \dot{z}_k = \beta f(y_k - z_k) + w_{k+1} - x_k \\ \dot{w}_k = \delta(y_k - z_{k+1}) \end{cases} \quad (1)$$

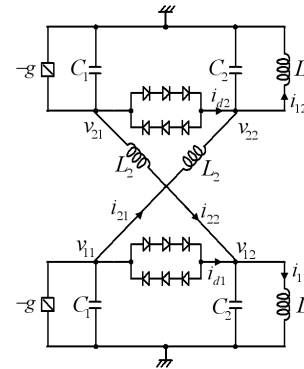


Figure 1: Basic circuit model.

where

$$\begin{cases} x_k = \sqrt{\frac{L_1}{C_2}} \frac{i_{k1}}{V}, & w_k = \sqrt{\frac{L_1}{C_2}} \frac{i_{k2}}{V}, \\ y_k = \frac{v_{k1}}{V}, & z_k = \frac{v_{k2}}{V}, & t = \sqrt{L_1 C_2} \tau, \\ \alpha = \frac{C_2}{C_1}, & \beta = \sqrt{\frac{L_1}{C_2}} G, & \gamma = \sqrt{\frac{L_1}{C_2}} g, \\ \delta = \frac{L_1}{L_2}, & \text{“,”} = \frac{d}{d\tau} \end{cases} \quad (2)$$

and z_3 indicates z_1 . The function f are nonlinear functions corresponding to the $v - i$ characteristics of the nonlinear resistors of the diodes and are described as follows.

$$f(y_k - z_k) = \begin{cases} y_k - z_k - 1 & (y_k - z_k > 1) \\ 0 & (|y_k - z_k| \leq 1) \\ y_k - z_k + 1 & (y_k - z_k < -1) \end{cases} \quad (3)$$

A typical example of the observed phenomena is shown in Fig. 2. Figure 2(a) is computer simulated results obtained by integrating Eq. (2) with the Runge-Kutta method and Fig. 2(b) is the corresponding circuit experimental results. In this state, the two circuits exhibited chaos but almost synchronized in in-phase in the sense that the attractor was almost in the quadrant I or III on the $y_1 - y_2$ (or $v_{11} - v_{21}$) plane. The behaviors of the circuits are very interesting because the solutions on the $y_i - z_i$ planes seem to be attracted to the fixed points located at around $(y_i, z_i) = (\pm 1.2, 0)$. However, after converging to the fixed points, the solution abruptly moves toward the other fixed point. When one circuit switches to/from the positive region

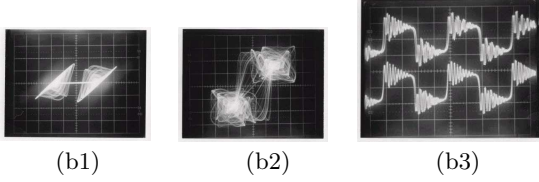
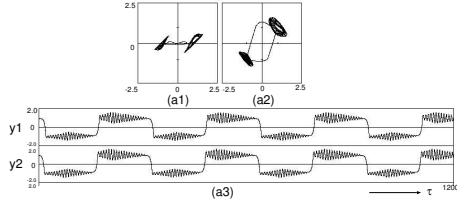


Figure 2: State transition phenomenon around in-phase synchronization. (a) Computer calculated results. $\alpha = 2.5$, $\beta = 4.0$, $\gamma = 0.1$, and $\delta = 0.0014$. (b) Circuit experimental results. $L_1 = 9.93\text{mH}$, $L_2 = 800\text{mH}$, $C_1 = 32.8\text{nF}$, and $C_2 = 49.5\text{nF}$, and $g = 683\text{mS}$. (a1) $y_1 - z_1$. (a2) $y_1 - y_2$. (a3) Time waveform. (b1) $v_{11} - v_{12}$. (b2) $v_{11} - v_{21}$. (b3) Time waveform v_{11} and v_{21} .

from/to the negative region in this way, the other follows the transition after a few instants.

By changing initial conditions, similar transition phenomena can be observed around anti-phase synchronization and quadrature-phase synchronization as shown in Fig. 3.

Figure 4 shows how the characteristics of the synchronization states change as the coupling parameter δ increases. The horizontal axis is δ and the vertical axis is the average length of the transitions and the delay time in τ . The curve of crosses shows the average period of the state transitions between positive and negative.

The curve of squares shows the average delay time of the state transitions of y_2 with respect to y_1 , when the anti-phase synchronization appears. While the curve of circles shows the average delay time of the state transitions of y_2 , when the quadrature-phase synchronization appears.

We can see that both anti-phase and quadrature-phase synchronizations coexist for a relatively wide parameter range.

3. Globally Cross-Coupled Chaotic Circuits

In this study, we consider a globally coupled system based on the cross-coupled circuits in Fig. 1. Namely, all n chaotic circuits are coupled to the others directly. Figure 5 shows the case of three circuits where R is small resistors introduced to avoid a loop of only inductors. In this case, the number of the connections from each node is two and each subcircuit has two nodes. Hence, the total number of the connections are $3 \times 2 \times 2/2 = 6$. Generally speaking, the total number of the connections of n coupled system is expressed as $n \times 2 \times (n-1)/2 = n(n-1)$.

By using the normalization similar to Eq. (1), the normalized circuit equations for the case of $n = 3$ are

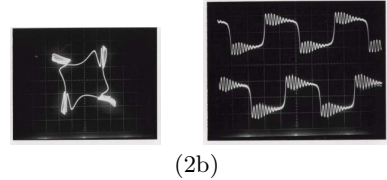
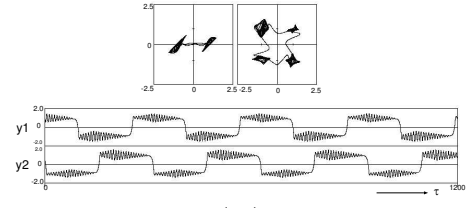
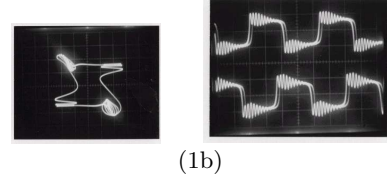
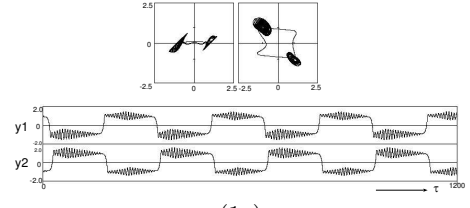


Figure 3: State transition phenomenon around (1) anti-phase synchronization and (2) quadrature-phase synchronization. (a) Computer calculated results. $\alpha = 2.5$, $\beta = 4.0$, $\gamma = 0.1$, and $\delta = 0.0014$. (b) Circuit experimental results. $L_1 = 9.93\text{mH}$, $L_2 = 1.2\text{H}$, $C_1 = 32.8\text{nF}$, $C_2 = 49.5\text{nF}$, and $g = 495\text{mS}$.

given as follows.

$$\begin{cases} \dot{x}_k = z_k & (k = 1, 2, 3) \\ \dot{y}_1 = \alpha \{ \gamma y_1 - w_1 - w_2 - \beta f(y_1 - z_1) \} \\ \dot{y}_2 = \alpha \{ \gamma y_2 - w_3 - w_6 - \beta f(y_2 - z_2) \} \\ \dot{y}_3 = \alpha \{ \gamma y_3 - w_4 - w_5 - \beta f(y_3 - z_3) \} \\ \dot{z}_1 = \beta f(y_1 - z_1) + w_4 + w_3 - x_1 \\ \dot{z}_2 = \beta f(y_2 - z_2) + w_2 + w_5 - x_2 \\ \dot{z}_3 = \beta f(y_3 - z_3) + w_1 + w_6 - x_3 \\ \dot{w}_1 = \delta(y_1 - z_3 - \epsilon w_1) \\ \dot{w}_2 = \delta(y_1 - z_2 - \epsilon w_2) \\ \dot{w}_3 = \delta(y_2 - z_1 - \epsilon w_3) \\ \dot{w}_4 = \delta(y_3 - z_1 - \epsilon w_4) \\ \dot{w}_5 = \delta(y_3 - z_2 - \epsilon w_5) \\ \dot{w}_6 = \delta(y_2 - z_3 - \epsilon w_6) \end{cases} \quad (4)$$

where ϵ is the parameter corresponding to the small resistors R .

4. Synchronization Patterns

Because the basic two cross-coupled circuits generates three types of synchronization states; in-phase, anti-phase, and quadrature-phase, we can expect the

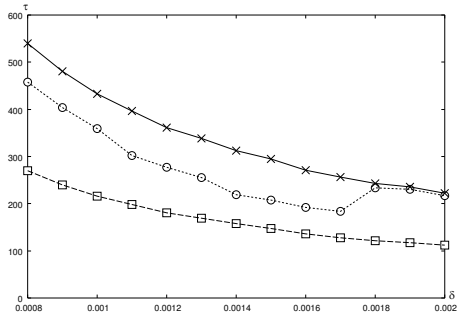


Figure 4: Characteristics of synchronization states. $\alpha = 2.5$, $\beta = 4.0$, and $\gamma = 0.1$.

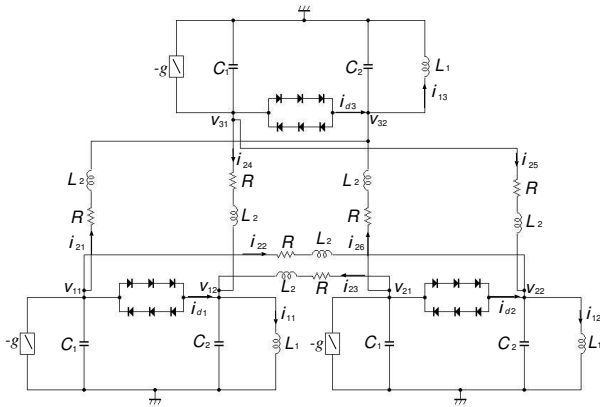


Figure 5: Three cross-coupled chaotic circuits.

generation of various types of synchronization patterns from the globally cross-coupled circuits.

4.1. Three subcircuits case

For the case of three subcircuits, the synchronization states can be expressed by the phase differences of y_2 and y_3 with respect to the reference waveform y_1 . For example, fully in-phase synchronization can be written as $[0, 0, 0]$. Also, if y_2 is synchronized to y_1 with $\pi/2$ phase difference (quadrature-phase) and y_3 is synchronized to y_1 with π phase difference (anti-phase), the state can be written as $[0, \pi/2, \pi]$. By using this notation, all possible combinations of the phase states can be summarized as

$$\begin{aligned}
 \text{TYPE I} &: [0, 0, 0] \\
 \text{TYPE II} &: [0, 0, \pi/2], [0, \pi/2, 0], [0, 0, -\pi/2], \\
 & [0, -\pi/2, 0], [0, \pi/2, \pi/2], [0, -\pi/2, -\pi/2] \\
 \text{TYPE III} &: [0, 0, \pi], [0, \pi, 0], [0, \pi, \pi] \\
 \text{TYPE IV} &: [0, \pi/2, \pi], [0, \pi, \pi/2], [0, \pi, -\pi/2], \\
 & [0, -\pi/2, \pi], [0, \pi/2, -\pi/2], [0, -\pi/2, \pi/2]
 \end{aligned} \quad (5)$$

Please note that all combinations in the same type can be obtained by using the symmetry of the coupling structure.

Figure 6 shows computer calculated results of the all possible types of synchronization states observed

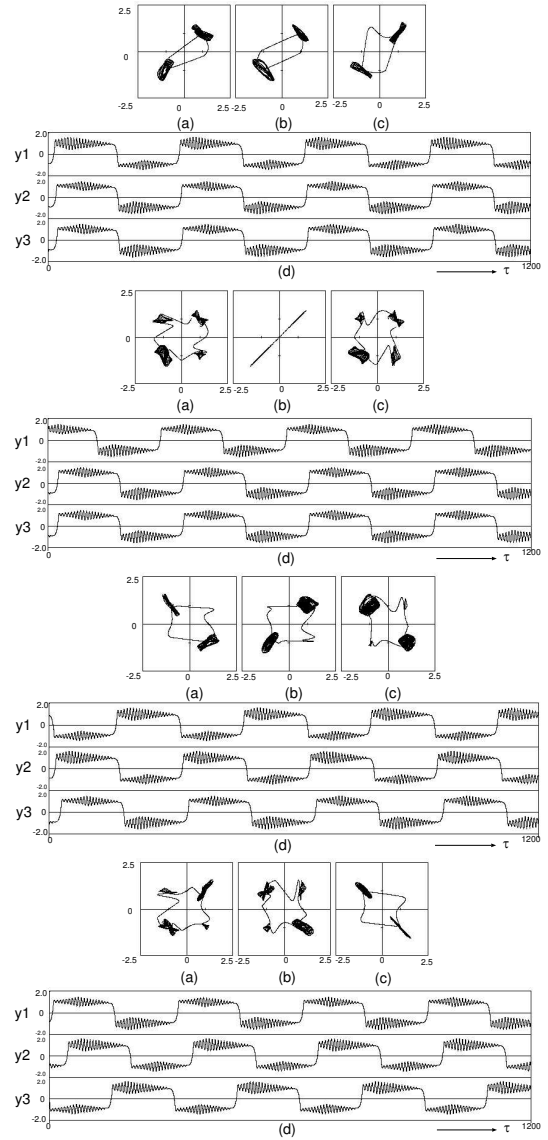


Figure 6: Four types of synchronization states (computer calculated result). $\alpha = 2.5$, $\beta = 4.0$, $\gamma = 0.1$, $\delta = 0.0007$, and $\epsilon = 0.0005$. From upper, TYPE I, II, III, and IV. (a) Attractor on $y_1 - y_2$ plane. (b) Attractor on $y_2 - y_3$ plane. (c) Attractor on $y_3 - y_1$ plane. (d) Time waveform.

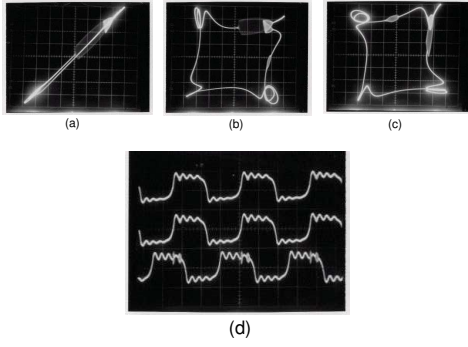


Figure 7: Circuit experimental result. $L_1 = 10.25\text{mH}$, $L_2 = 1.5\text{H}$, $C_1=32.2\text{nF}$, $C_2=49.5\text{nF}$, and $g=512\text{mS}$. (a) Attractor on $v_{11} - v_{12}$ plane. (b) Attractor on $v_{12} - v_{13}$ plane. (c) Attractor on $v_{13} - v_{11}$ plane. (d) Time waveform v_{11} and v_{21} .

from the three cross-coupled circuits. Please note that the coupling parameter δ is a half of the case of the two circuits in Figs. 2 and 3. This is because the number of the connections are doubled. Figure 7 shows an example of circuit experimental results (TYPE II).

4.2. Four subcircuits case

For the case of four subcircuits, all possible types of the synchronization states can be summarized using the same notation as follows;

$$\begin{aligned}
 \text{TYPE I :} & \quad [0, 0, 0, 0] \\
 \text{TYPE II :} & \quad [0, 0, 0, \pi/2] \\
 \text{TYPE III :} & \quad [0, 0, 0, \pi] \\
 \text{TYPE IV :} & \quad [0, 0, \pi/2, \pi/2] \\
 \text{TYPE V :} & \quad [0, 0, \pi, \pi] \\
 \text{TYPE VI :} & \quad [0, 0, \pi/2, \pi]
 \end{aligned} \tag{6}$$

All other combinations of phase states can be obtained from these type by using the symmetry of the coupling structure.

Figures 8 shows computer calculated results of the all possible types of synchronization states. As similar to the previous case, the coupling parameter δ is one third of the case of the two circuits in Figs. 2 and 3.

5. Conclusions

In this study, we have investigate the synchronization patterns characterized by the synchronization states in globally cross-coupled chaotic circuits. We confirmed that several patterns could be observed by giving different initial conditions to the circuits for the cases of the number of the circuits are three and four. Our future research includes the investigation of the larger size circuits, the clarification of the generation mechanism of the transition, and the application to signal processing using the proposed circuit.

Acknowledgments

This work was partly supported by Yazaki Memorial Foundation for Science and Technology.

References

[1] Ch. von der Malsburg and J. Buhmann, "Sensory Segmentation with Coupled Neural Oscillators," *Biol. Cybern.*, vol. 67, pp. 233-242, 1992.

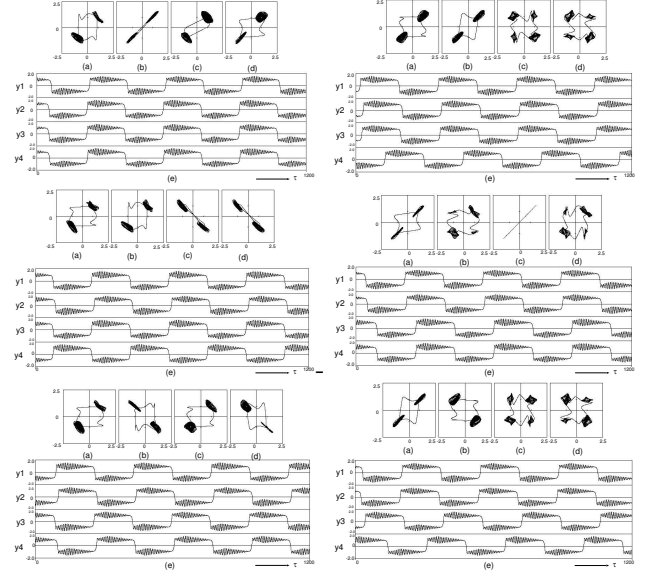


Figure 8: Six types of synchronization states (computer calculated result). $\alpha = 2.5$, $\beta = 4.0$, $\gamma = 0.1$, $\delta = 0.00046$, and $\epsilon = 0.0005$. From upper-left, TYPE I, II, III, IV, V, and VI. (a) Attractor on $y_1 - y_2$ plane. (b) Attractor on $y_2 - y_3$ plane. (c) Attractor on $y_3 - y_4$ plane. (d) Attractor on $y_4 - y_1$ plane. (e) Time waveform.

[2] S. Campbell and D. Wang, "Synchronization and Desynchronization in a Network of Locally Coupled Wilson-Cowan Oscillators," *IEEE Trans. Neural Networks*, vol. 7, no. 3, pp. 541-553, Mar. 1996.

[3] G. Abramson, V.M. Kenkre and A.R. Bishop, "Analytic Solutions for Nonlinear Waves in Coupled Reacting Systems," *Physica A*, vol. 305, no. 3-4, pp. 427-436, 2002.

[4] I. Belykh, M. Hasler, M. Lauret and H. Nijmeijer, "Synchronization and Graph Topology," *Int. J. Bifurcation and Chaos*, vol. 15, no. 11, pp. 3423-3433, 2005.

[5] Y. Uchitani, R. Imabayashi and Y. Nishio, "State Transition Phenomenon in Cross-Coupled Chaotic Circuits," *Proc. of NOLTA'07*, pp. 397-400, Sep. 2007.

[6] Y. Uchitani and Y. Nishio, "Investigation of State Transition Phenomena in Cross-Coupled Chaotic Circuits," *Proc. of ISCAS'08*, pp. 2394-2397, May. 2008.

[7] Y. Uchitani and Y. Nishio, "Synchronization Patterns Generated in a Ring of Cross-Coupled Chaotic Circuits," *Proc. of IJCNN'08*, pp. 3854-3859, Jun. 2008.

[8] M. Shinriki, M. Yamamoto and S. Mori, "Multimode Oscillations in a Modified van der Pol Oscillator Containing a Positive Nonlinear Conductance," *Proc. of IEEE*, vol. 69, pp. 394-395, 1981.

[9] N. Inaba, T. Saito and S. Mori, "Chaotic Phenomena in a Circuit with a Negative Resistance and an Ideal Switch of Diodes," *Trans. of IEICE*, vol. E70, no. 8, pp. 744-754, 1987.